

Zeeman decoherence effect of trapped $^{199}Hg^{+}$ ion Ramsey spectra

Ge Liu(刘格), Hao Liu(柳浩), Yihe Chen(陈义和), Jian Wang(王健), Shuhong Huang(黄书泓), Chengbin Li(李承斌), and Lei She(佘磊)

Citation: Chin. Phys. B, 2024, 33 (**11**): 113702. DOI: 10.1088/1674-1056/ad7af6
Journal homepage: http://cpb.iphy.ac.cn; http://iopscience.iop.org/cpb

What follows is a list of articles you may be interested in

A cryogenic radio-frequency ion trap for a $^{40}Ca^{+}$ optical clock

Mengyan Zeng(曾孟彦), Yao Huang(黄垚), Baolin Zhang(张宝林), Zixiao Ma(马子晓), Yanmei Hao(郝艳梅), Ruming Hu(胡如明), Huaqing Zhang(张华青), Hua Guan(管桦), and Kelin Gao(高克林)
Chin. Phys. B, 2023, 32 (**11**): 113701. DOI: 10.1088/1674-1056/acc807

Numerical analysis of motional mode coupling of sympathetically cooled two-ion crystals

Li-Jun Du(杜丽军), Yan-Song Meng(蒙艳松), Yu-Ling He(贺玉玲), and Jun Xie(谢军)
Chin. Phys. B, 2021, 30 (**7**): 073702. DOI: 10.1088/1674-1056/abfc3e

Setup of a dipole trap for all-optical trapping

Miao Wang(王淼), Zheng Chen(陈正), Yao Huang(黄垚), Hua Guan(管桦), and Ke-Lin Gao(高克林)
Chin. Phys. B, 2021, 30 (**5**): 053702. DOI: 10.1088/1674-1056/abd767

Optimization of endcap trap for single-ion manipulation

Yuan Qian(钱源), Chang-Da-Ren Fang(方长达人), Yao Huang(黄垚), Hua Guan(管桦), Ke-Lin Gao(高克林)
Chin. Phys. B, 2018, 27 (**6**): 063701. DOI: 10.1088/1674-1056/27/6/063701

Quantitative evaluation of space charge effects of laser-cooled three-dimensional ion system on a secular motion period scale

Li-Jun Du(杜丽军), Hong-Fang Song(宋红芳), Shao-Long Chen(陈邵龙), Yao Huang(黄垚), Xin Tong(童昕), Hua Guan(管桦), Ke-Lin Gao(高克林)
Chin. Phys. B, 2018, 27 (**4**): 043701. DOI: 10.1088/1674-1056/27/4/043701

Zeeman decoherence effect of trapped $^{199}Hg^+$ ion Ramsey spectra

Ge Liu(刘格)[1,2], Hao Liu(柳浩)[1,†], Yihe Chen(陈义和)[1], Jian Wang(王健)[1,2], Shuhong Huang(黄书泓)[1,2], Chengbin Li(李承斌)[1,3], and Lei She(佘磊)[1,‡]

[1] *Key Laboratory of Atomic Frequency Standards (KLAFS), Innovation Academy for Precision Measurement Science and Technology, Chinese Academy of Sciences, Wuhan* 430071, *China*

[2] *University of Chinese Academy of Sciences, Beijing* 100049, *China*

[3] *State Key Laboratory of Magnetic Resonance and Atomic and Molecular Physics, Innovation Academy for Precision Measurement Science and Technology, Chinese Academy of Sciences, Wuhan* 430071, *China*

(Received 14 June 2024; revised manuscript received 5 September 2024; accepted manuscript online 14 September 2024)

In the $^{199}Hg^+$ ion microwave clock, the Zeeman decoherence effect caused by the overlapping of Zeeman sidebands and the radial secular motion sidebands will decrease the contrast of the Ramsey fringe, thus reducing the signal-to-noise ratio of the spectra. In this paper, the Zeeman decoherence effect is analyzed theoretically and investigated experimentally. A simplified model is built to describe the Ramsey spectral probability, in which the transverse relaxation time T_2 is introduced to characterize the influence of the Zeeman decoherence effect phenomenologically. The experiments were carried out on a linear quadrupole trap $^{199}Hg^+$ ion clock. The results show that the probability model matches well with the experimental data, and the magnetic field value should be more than 150 mGs (1 Gs = 10^{-4} T) to avoid the Zeeman decoherence effect.

Keywords: $^{199}Hg^+$ ion microwave clock, Zeeman decoherence, transverse relaxation time

PACS: 37.10.Ty, 32.10.Fn, 32.30.–r **DOI:** 10.1088/1674-1056/ad7af6

1. Introduction

Atomic clocks are the most accurate time–frequency standard known in the world. Atomic clocks are widely used in scientific research and engineering technology fields such as timekeeping,[1,2] satellite navigation,[3] and deep space exploration.[4] The $^{199}Hg^+$ ion microwave clock is based on using ion trap technology, ^{202}Hg ultraviolet (UV) discharge lamp pumping, and buffer gas cooling, making it lightweight, small volume, simple structure, and good reliability. The $^{199}Hg^+$ ion microwave clock exhibits low second-order Doppler shift,[5,6] suitable for miniaturization,[7] and low environmental sensitivity,[8] making it an ideal choice for the next generation of space clock and timekeeping clock.[9,10]

Due to the inevitable coupling between the atomic system and the surrounding environment, such as spontaneous emission, magnetic field noise,[11] spin-exchange collisions,[12] and collision,[13] etc., it will cause the decoherence of the quantum system. The decoherence will lead to a rapid dephasing of the system's wave function and consequently affect the transition frequency in research areas such as ultracold atomic ensembles,[14] superconducting devices,[15] and nitrogen–vacancy centers in diamond.[16,17] The advantage of the $^{199}Hg^+$ ion microwave clock is that there are no wall collisions to repopulate a state-prepared two-level ion (T_1 relaxation) or to destroy atomic coherence (T_2 relaxation),[18] so very high resolution can be achieved. The short-term stability performance of the $^{199}Hg^+$ ion microwave clock is determined by Allan variance $\sigma = \frac{1}{\pi(\mathrm{SNR})Q}\sqrt{T_c/t}$, where t is the averaging time, T_c is the cycle time, SNR is the signal-to-noise ratio, the quality factor $Q = \upsilon_0/\Delta\upsilon$, where $\Delta\upsilon$ is the central Ramsey fringe width and $\upsilon_0 = 40.5$ GHz. The $\mathrm{SNR} = (S/2)/\sqrt{S/2+B}$, where S is the signal size measured at the maximum point, B is the amount of background collected light not contributing to the signal. However, the Zeeman decoherence effect caused by the overlapping of the Zeeman sidebands and radial secular motion sidebands of $^{199}Hg^+$ ions could decrease the contrast of Ramsey fringes.[19] The SNR is proportional to the contrast of the Ramsey fringe which is defined as the ratio of the difference between the maximum and minimum values of the fringes to their sum, meaning that the Zeeman decoherence effect negatively impacts the performance of the $^{199}Hg^+$ ion microwave clock. Previously, to increase the SNR, the free evolution time is appropriately reduced, and then the trapping ions experience a shorter decoherence process during the two $\pi/2$ microwave pulses.[20] The center line width is broader, though the SNR will increase.

In this paper, we conduct a theoretical analysis and experimental exploration of the impact of the Zeeman decoherence effects on Ramsey spectra measurements within a linear quadrupole $^{199}Hg^+$ ion microwave clock. Our numerical analysis focuses on the relationship between magnetic field sidebands, secular motion sidebands, and transverse relaxation time T_2. Furthermore, we give a simple description of a Ramsey fringe subject to T_2, and obtain the minimum value of

†Corresponding author. E-mail: liuhao@apm.ac.cn

‡Corresponding author. E-mail: shelei@apm.ac.cn

© 2024 Chinese Physical Society and IOP Publishing Ltd

the magnetic field setting from the experiment to increase the SNR. Finally, we discuss how to avoid the Zeeman decoherence effect.

2. Experiment principle and setups

The $^{199}Hg^{+}$ ion microwave clock operates as a passive frequency standard, using the ground state hyperfine transition frequency of $^{199}Hg^{+}$ as its reference. The energy level diagram of $^{199}Hg^{+}$ ions and the experimental setup are shown in Fig. 1. The $^{199}Hg^{+}$ ions are confined in a linear quadrupole trap by applying radio-frequency (RF) voltage to the poles. The 194.2-nm light emitted by the ^{202}Hg discharge lamp excites the trapped $^{199}Hg^{+}$ ions in the ground state $^{2}S_{1/2}$ $(F = 1)$ to the $^{2}P_{1/2}$ state. Ions in the $^{2}P_{1/2}$ state are unstable and will spontaneously radiate back to the $^{2}S_{1/2}$ $(F = 0)$ and $^{2}S_{1/2}$ $(F = 1)$ states, simultaneously emitting fluorescence. After a period of pumping, almost all ions are in the $^{2}S_{1/2}$ $(F = 0)$ state, and the fluorescence disappears, indicating that the optically pumped state selection process is realized. Then the 40.5-GHz microwave is radiated to the ions, and the ions take place resonance transition from the $^{2}S_{1/2}$ $(F = 0)$ state to the $^{2}S_{1/2}$ $(F = 1)$ state. At this time, if the ions are illuminated with the ^{202}Hg lamp, the fluorescence will be observed again. The fluorescence is collected by a photomultiplier tube (PMT). The actual count is equal to the ion numbers (signal size) multiplied by the transition probability and then added to the background count. A Helmholtz coil centered on the trapping region is used to apply the C-field (constant field) quantization axis. To prevent ambient field disturbances from influencing the ion hyperfine frequency, the trap region is surrounded by a triple layer magnetic shield.

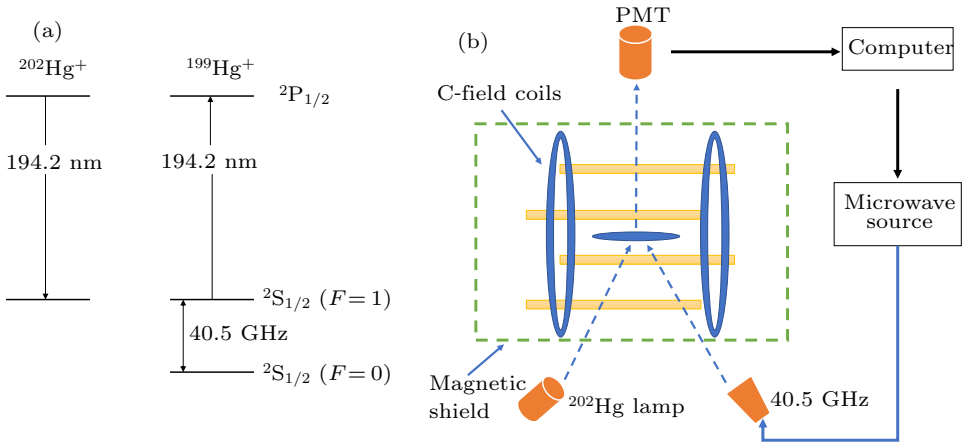


Fig. 1. (a) Hg^{+} energy level diagram. (b) Schematic experimental setup.

3. Zeeman decoherence effect

For $^{199}Hg^{+}$, the nuclear spin $I = 1/2$, $F = 1$ states generate Zeeman splitting as shown in Fig. 2. The ground state hyperfine transition spectrum will exhibit three peaks which correspond to the transitions from $^{2}S_{1/2}$ $(F = 0,\ m_F = 0)$ state to $^{2}S_{1/2}$ $(F = 1,\ m_F = 1)$ state, $^{2}S_{1/2}$ $(F = 0,\ m_F = 0)$ state to $^{2}S_{1/2}$ $(F = 1,\ m_F = 0)$ state, and $^{2}S_{1/2}$ $(F = 0,\ m_F = 0)$ state to $^{2}S_{1/2}$ $(F = 1,\ m_F = -1)$ state. This phenomenon is the first-order Zeeman effect, with the corresponding frequency given by

$$\nu' = \nu_0 + \begin{cases} \dfrac{e}{4\pi m_e}B, \\ 0, \\ -\dfrac{e}{4\pi m_e}B, \end{cases} \tag{1}$$

where υ_0 is the clock transition frequency without disturbance, $e/(4\pi m_e) = 1.4\ \mathrm{MHz/Gs}$ $(1\ \mathrm{Gs} = 10^{-4}\ \mathrm{T})$. There is a second-order Zeeman effect for the clock transition from $^{2}S_{1/2}$ $(F = 0,\ m_F = 0)$ state to $^{2}S_{1/2}$ $(F = 1,\ m_F = 0)$ state:[19]

$$\nu = \nu_0 + 97.2B^2\ [\mathrm{Hz/Gs^2}]. \tag{2}$$

Assume M is the magnetic shielding factor, B_A is the magnitude of the ambient magnetic field, B_c is the magnetic field generated by the C-field coils. Then the total magnetic field is $B = (B_A/M) + B_c$. According to formula (2), the second-order Zeeman frequency shift is $\delta\nu = 2 \times 97.2 \times B \times \delta B$, where δB is mainly determined by the variation of the C-field coil current source. Because of the large magnetic shielding factor M and the fine C-field power supply, the size of the B_c greatly affects the magnetic field frequency shift. The second-order Zeeman frequency shift, the second-order Doppler frequency shift, and the buffer gas collision frequency shift are the three primary factors affecting the frequency stability of the $^{199}Hg^{+}$ ion microwave clock.[21]

To realize the clock transition $(\Delta m_F = 0)$ from the $^{2}S_{1/2}$ $(F = 0,\ m_F = 0)$ state to the $^{2}S_{1/2}$ $(F = 1,\ m_F = 0)$ state in the $^{199}Hg^{+}$ ion microwave clock, the direction of the microwave magnetic field component and the C-field should be set parallel. The microwave radiation direction is perpendicular to the axis of the trap, ensuring that the ion motion in this direction is less than the microwave's wavelength, satis-

fying the "Lamb–Dick" requirement.[22] However, in practice, the direction of microwave radiation may not be perfectly perpendicular to the axis of the trap. In addition, the length of the ion trap is long, which means that the microwave propagation direction will diverge during transmission. Hence, there will be a magnetic field component of the microwave radiation which is parallel with the radial direction of the ion trap, and the allowed transitions obey $\Delta m_F = \pm 1$.

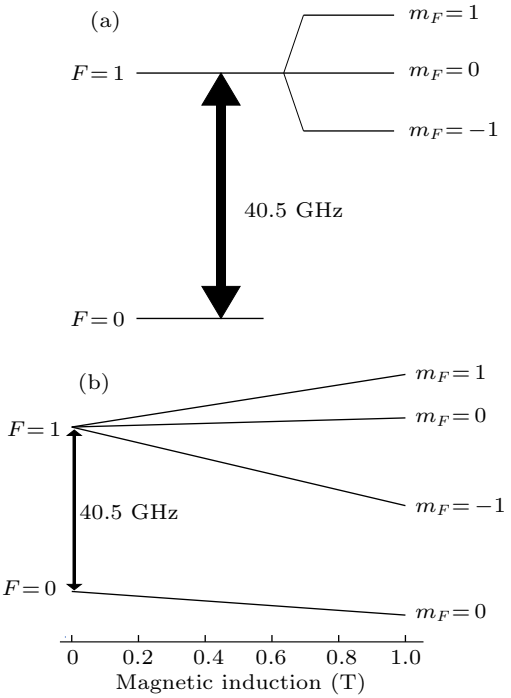


Fig. 2. (a) The ground state hyperfine level structure of $^{199}Hg^{+}$ and (b) magnetic effects.

The ions are trapped in a linear quadrupole trap, where their radial motion can be approximated as simple harmonic motion. Because of the Doppler effect, the trapped ions will have two radial secular motion sidebands, which are about tens of kHz away from the center frequency. When microwave resonance is performed, the microwave angular frequency seen by the ions in the radial direction is $\omega_0 \pm \omega_D$ (ω_0 is the clock transition center frequency, ω_D is the radial secular motion frequency). If the Zeeman sidebands overlap with the radial secular motion sidebands, then the ions will undergo not only the $\Delta m_F = 0$ transition, but also the transitions with $\Delta m_F = 1$ and $\Delta m_F = -1$, which leads to the decoherence of the Ramsey process and causes spectrum deformation.

The Zeeman decoherence effect can be illustrated with the concept of transverse relaxation time T_2. Considering a two-level system interacts with an optical field, when the interrogation field is switched off, different relaxation processes can affect the phase relationship between different oscillating atomic dipoles.[23] The density matrix is

$$\rho = \begin{pmatrix} \rho_{11} & \rho_{12} \\ \rho_{21} & \rho_{22} \end{pmatrix}. \tag{3}$$

The diagonal elements ρ_{11} and ρ_{22} represent the time-dependent population densities and the off-diagonal elements ρ_{12} and ρ_{21} represent coherences. T_2 relaxation is the additional relaxation to the coherent terms or non-diagonal terms of the density matrix. T_1 is the longitudinal relaxation time, which represents the process of changing the number of particles. T_2 relaxation generally proceeds more rapidly than T_1 recovery. When the Zeeman sidebands overlap with the secular motional sidebands, the coherence of ions is destroyed (T_2 relaxation).

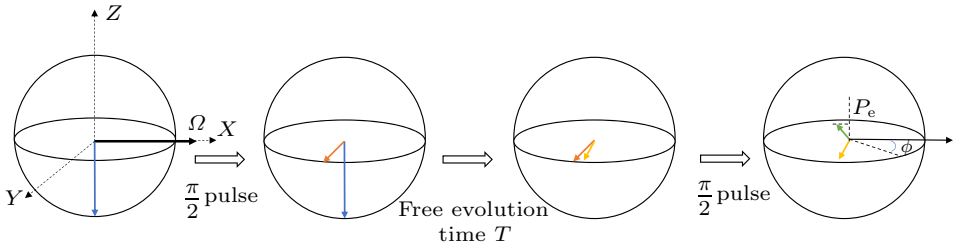


Fig. 3. The Bloch sphere and Ramsey time sequence. Initially, the ion is in the lower energy level, with its magnetic moment directed along the negative direction of the z axis. A $\pi/2$ pulse is then applied, which causes the magnetic moment to rotate 90° around the x axis to the XY plane. During the free evolution time T, the magnetic moment rotates around the z axis on the XY plane. A second $\pi/2$ pulse is applied, and the magnetic moment rotates another 90° around the x axis. Ultimately, the projection of the magnetic moment onto the z axis corresponds to the probability of the ion transitioning from the lower to the upper energy level.

The microwave resonance time sequence for measuring the Ramsey spectra is illustrated in Fig. 3: two $\pi/2$ pulses, each with a duration of τ, are applied to the ions with an interval of T. Assuming that the atom is initially in the lower energy level $|1\rangle$ state, the probability of measuring an atom in the upper energy level $|2\rangle$ state can be approximated as follows:[24]

$$P(2\tau + T) \approx \frac{1}{2}\left[1 + \cos(\omega - \omega_0)T\right]\sin^2\Omega\tau. \tag{4}$$

Among them, $\Omega = \sqrt{(\omega - \omega_0)^2 + (\Omega')^2}$ is the Rabi oscillation frequency, where $\omega - \omega_0$ is the detuning, and $\Omega' = H_0\mu/\hbar$ is proportional to the product of the magnetic field amplitude H_0 of the microwave pulse and the transition magnetic dipole moment μ of the atom. The central Ramsey fringe width $\Delta\nu \approx 1/(2T)$, and $\nu = \omega/(2\pi)$. The formula (4) can be decomposed into the Rabi part $\sin^2\Omega\tau$ and the Ramsey interference part $\frac{1}{2}\left[1 + \cos(\omega - \omega_0)T\right]$ which could be considered as

the modulation of the transition probability amplitude caused by the interference of two separated microwave fields. After the first $\pi/2$ pulse, the spin is out of phase due to the local microscopic field inhomogeneity, resulting in signal loss. The decay of magnetization within the XY plane takes an exponential process (e^{-T/T_2}). Use the Bloch sphere to calculate the Ramsey probability under relaxation

$$P_2(\phi,T) = \langle 2|\mathrm{e}^{\mathrm{i}\frac{\pi}{4}\boldsymbol{e}_\phi\cdot\boldsymbol{\sigma}}\hat{\rho}(T)\,\mathrm{e}^{-\mathrm{i}\frac{\pi}{4}\boldsymbol{e}_\phi\cdot\boldsymbol{\sigma}}|2\rangle, \tag{5}$$

where $\boldsymbol{\sigma}$ is the Pauli operator, ϕ is phase evolution.

$$\begin{aligned}\mathrm{e}^{-\mathrm{i}\frac{\pi}{4}\boldsymbol{e}_\phi\cdot\boldsymbol{\sigma}}|2\rangle &= \left[\cos\frac{\pi}{4}\hat{1} - \mathrm{i}(\cos\phi\,\hat{\sigma}_x + \sin\phi\,\hat{\sigma}_y)\sin\frac{\pi}{4}\right]|2\rangle \\ &= \frac{1}{\sqrt{2}}(\hat{1} - \mathrm{i}\,\mathrm{e}^{-\mathrm{i}\phi}\hat{\sigma}_+ - \mathrm{i}\,\mathrm{e}^{\mathrm{i}\phi}\hat{\sigma}_-)|2\rangle \\ &= \frac{1}{\sqrt{2}}(|2\rangle - \mathrm{i}\,\mathrm{e}^{\mathrm{i}\phi}|1\rangle), \end{aligned}\tag{6}$$

$$\begin{aligned}P_2(\phi,T) &= \frac{1}{2}\big[\rho_{22}(T) + \rho_{11}(T) - \mathrm{i}\,\mathrm{e}^{\mathrm{i}\phi}\rho_{21}(T) \\ &\quad - \mathrm{i}\,\mathrm{e}^{-\mathrm{i}\phi}\rho_{12}(T)\big]. \end{aligned}\tag{7}$$

Here $\rho_{22}(T) + \rho_{11}(T) = 1$

$$\begin{aligned}P_2(\phi,T) &= \frac{1}{2}[1 - 2\,\mathrm{Im}(\rho_{21}(T))\cos\phi \\ &\quad + 2\,\mathrm{Re}(\rho_{12}(T))\sin\phi]. \end{aligned}\tag{8}$$

Setting $T = 0$, $\phi = 0$

$$|\psi\rangle = \mathrm{e}^{-\mathrm{i}\frac{\pi}{4}\hat{\sigma}_x}|1\rangle = \frac{1}{\sqrt{2}}(|1\rangle - \mathrm{i}|2\rangle), \tag{9}$$

$$\rho_{21}(0) = -\frac{\mathrm{i}}{2}, \quad \rho_{12}(0) = \frac{\mathrm{i}}{2}. \tag{10}$$

Then when $T \geq 0$, introducing the relaxation term e^{-T/T_2}

$$\rho_{21}(T) = \rho_{21}(0)\,\mathrm{e}^{-T/T_2} = -\frac{\mathrm{i}}{2}\mathrm{e}^{-T/T_2}. \tag{11}$$

Get

$$P_2(\phi,T) = \frac{1}{2}\left(1 + \mathrm{e}^{-T/T_2}\cos\phi\right). \tag{12}$$

As shown in Fig. 4(a), the contrast of Ramsey fringes decreases as the T_2 decreases, where the T_2 values corresponding to the black, red, and blue lines decrease in turn. The Ramsey spectra are obtained by scanning microwave pulses with detuning Δ and $\Phi = \Delta \times T$, where $\Delta = \omega - \omega_0$, ω_0 is the atomic transition center frequency, and ω is the microwave angular frequency. Then for the $^{199}\mathrm{Hg}^+$ ion microwave clock, the probability of ions transition from $^2\mathrm{S}_{1/2}$ ($F = 0$, $m_F = 0$) to $^2\mathrm{S}_{1/2}$ ($F = 1$, $m_F = 0$) is formula (12) multiplied by Rabi term as shown in Fig. 4(b)

$$\begin{aligned}&P(F = 1,\, m_F = 0) \\ &= \frac{1}{2}\left[1 + \mathrm{e}^{-T/T_2}\cos(\omega - \omega_0)T\right]\sin^2\Omega\tau. \end{aligned}\tag{13}$$

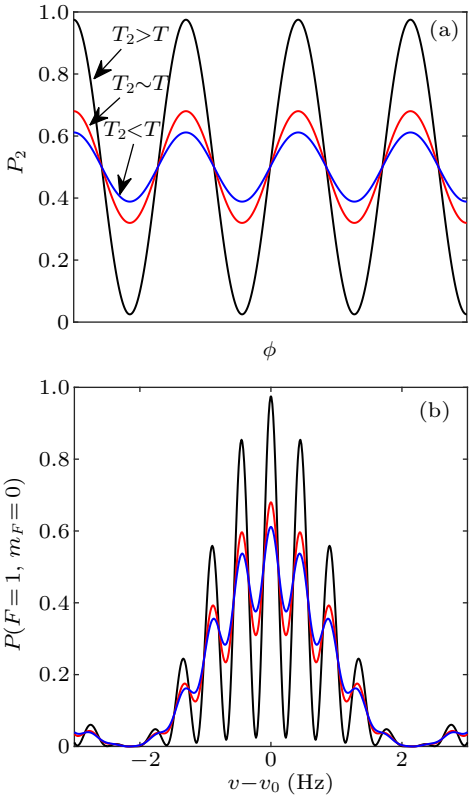


Fig. 4. (a) Ramsey fringe contrast for different T_2. (b) The probability of ions transition from $^2\mathrm{S}_{1/2}$ ($F = 0$, $m_F = 0$) to $^2\mathrm{S}_{1/2}$ ($F = 1$, $m_F = 0$) for different T_2.

Then we made relevant experiments on a quadrupole trap system by applying varying magnetic field magnitudes. First of all, the sideband spectra of $^{199}\mathrm{Hg}^+$ ions were scanned with the microwave–optical double resonance method. The four pictures [(a)–(d)] on the left of Fig. 5 show five peaks, which are respectively the central frequency peak, two radial secular motion sidebands, and two Zeeman sidebands. Next, the Ramsey spectra were scanned as shown by the black dots in four pictures [(e)–(h)] on the right side of Fig. 5, with the free evolution time of $T = 2.2$ s. Each time we change the magnetic field magnitude B_c, the center frequency would move slightly according to formula (2).

The analysis of the four sets of experimental data reveals that when the RF voltage applied to the ion trap poles is fixed, the radial secular motion sideband frequency remains unchanged at ±45 kHz. The Zeeman sidebands are first-order Doppler broadened with a width of tens of kHz. Initially, when the magnetic field is small, the Zeeman sidebands and the secular motion sidebands overlap completely, and the scanned Ramsey fringe contrast is 0. With the increase of the magnetic field, the Zeeman sideband and the secular motion sideband gradually separate, leading to an increase in the Ramsey fringe contrast. The Ramsey fringe contrast of picture (h) is close to 1.

Transverse relaxation decay is used to phenomenally describe the decrease in Ramsey fringe contrast caused by the Zeeman decoherence effect. However, formula (13) does not

match our experimental results. The clock transition of the $^{199}Hg^{+}$ ion microwave clock is $^{2}S_{1/2}$ $(F=0,\ m_F=0)$ to $^{2}S_{1/2}$ $(F=1,\ m_F=0)$. However, when the microwave clock uses a ^{202}Hg lamp for light pumping and fluorescence detection, the spectral range of the ^{202}Hg lamp is relatively wide, and the three sub-energy levels of $^{2}S_{1/2}$ $(F=1,\ m_F=0,\ \pm1)$ cannot be distinguished. Therefore, the $^{2}S_{1/2}$ $(F=1,\ m_F=\pm1)$ state ions are also excited to the $^{2}P_{1/2}$ state, then spontaneously radiate to the $^{2}S_{1/2}$ $(F=0)$ state, participating in the next optical pumping–microwave resonance–fluorescence detection cycle. The measured fluorescence counts are the sum of the population numbers on the three sub-energy levels. A comparison of pictures [(f)–(h)] reveals that while the Zeeman decoherence effect changes the population probability at the three hyperfine energy levels, it does not change the number of ions transitioning between the upper and lower hyperfine levels in the ground state, thereby maintaining a constant Rabi envelope. At the detuning is 0, the transition probability is 1.

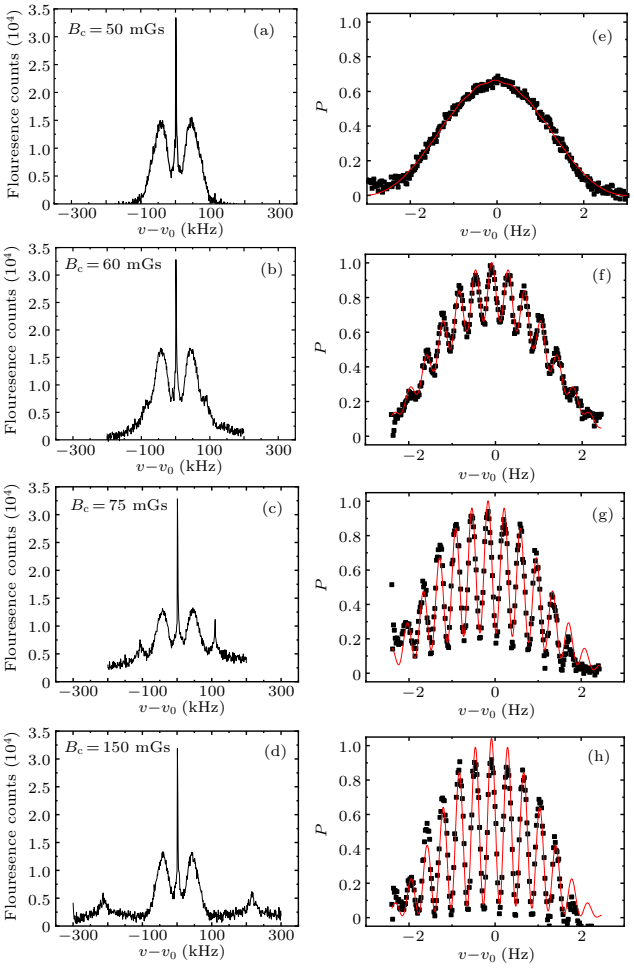


Fig. 5. The left depicts the sideband spectra of $^{199}Hg^{+}$ ions, with each picture showing 5 peaks: the central peak, two secular motion sidebands, and two Zeeman sidebands. The right presents the corresponding Ramsey spectra, wherein the black points are experimental data and the red lines are fitting lines. As the magnetic field increases, the Ramsey fringe contrast gradually increases.

We can regard the three sub-levels of $^{2}S_{1/2}$ $(F=1)$ as a whole, thereby considering $^{2}S_{1/2}$ $(F=0)$ state and $^{2}S_{1/2}$ $(F=1)$ state as two-level systems. Consequently, we introduce addition terms with unknown coefficient to the formula (13) to get the probability that ions transition to the upper energy level $^{2}S_{1/2}$ $(F=1)$, where the relaxation factor is denoted as e^{-T/T_2}. Furthermore, experimental images suggest that the decay of the amplitude modulation in Ramsey interference results in the probability function adopting the following form:

$$P(F=1)\approx\frac{1}{2}\left[A+Be^{-T/T_2}+Ce^{-T/T_2}\cos\phi\right]\sin^2\Omega\tau. \quad (14)$$

By fitting the formula (14) with the experimental data, the results show that coefficients A, B, and C are 2, -1, and 1, respectively. Moreover, the microwave resonance time τ, free evolution time T, signal size, and background counts obtained by each group of fitting are consistent. So, the fitting is very successful and then obtain

$$P(F=1)\approx\frac{1}{2}\left[1+\left(1-e^{-T/T_2}\right)+e^{-T/T_2}\cos\phi\right]\sin^2\Omega\tau. \quad (15)$$

The experimental data is fitted using the formula (15). As shown in Figs. 5(f)–5(h), the black dots are the experimental data, and the red lines are the fitting lines. Obviously, they match well. Based on the fitting results, the values of T_2 corresponding to pictures [(f)–(h)] are 2.38 s, 9.7 s, and 34.8 s respectively.

4. Discussion

The formula (15) provides an approximate expression that allows us to understand the impact of the length of ion coherence time on the transition spectrum. The fitting results reveal that when the magnetic field is small and the Zeeman sidebands completely overlap with the secular motion sidebands as shown in Fig. 5(a), the transverse relaxation time T_2 is very short, leading to the disappearance of Ramsey fringe. This indicates a loss of coherence, resulting in a Rabi line shape for the spectrum, as shown in Fig. 5(e). And the maximum probability is less than the other three pictures, indicating that T_1 is shorter. When the magnetic field increases, the Zeeman sidebands gradually move away from the secular motion sidebands, causing T_2 to increase and the fringe contrast to rise. As the magnetic field reaches 150 mGs as shown in Fig. 5(d), the T_2 is long and the fringe contrast approaches 1, indicating that the Zeeman decoherence effect has been nearly eliminated. According to the experimental results and analysis, we can see that the contrast of the Ramsey spectrum is positively related to transverse relaxation time T_2. When the secular motion sideband frequency is unchanged, a larger magnetic field results in a longer T_2 time. Given that the SNR is proportional to the contrast of the Ramsey spectrum, suppressing the Zeeman decoherence effect is crucial for achieving high performance in the $^{199}Hg^{+}$ ion microwave clock. This requires setting the magnetic field to more than 150 mGs. What is more,

$T_2 = 34.8$ s is significantly greater than the free evolution time $T = 2.2$ s, suggesting that it is feasible to appropriately increase T in future experiments to further narrow the Ramsey center line width.

The analysis of the location of Zeeman sidebands and secular motion sidebands can inform the selection of optimal experimental parameters. There are mainly two ways to avoid the Zeeman decoherence effect: one is increasing the magnetic field, and the other is decreasing the secular motion sideband frequency. However, an excessively high magnetic field can lead to a significant second-order Zeeman frequency shift. Therefore, we need to find the balanced value of the magnetic field through experiments to ensure that the second-order Zeeman frequency shift is small and the Zeeman decoherence can be avoided. If one wants to change the secular motion sideband frequency, it will be important to control the ion trap RF voltage, ion cloud temperature, and background gas pressure. We can analyze the line widths and location of the Zeeman sideband and motion sideband, from which we can get information about the number of ions and the temperature.[22,25] Armed with that information, we can get a better performance of the $^{199}Hg^{+}$ ion microwave clock probably.

5. Conclusion

In this paper, we conduct a theoretical analysis and experimental investigation of the Ramsey spectral probability model for the $^{199}Hg^{+}$ ions microwave clocks subject to the Zeeman decoherence effect. The results show that the experimental data match well with the derived formula. We use the transverse relaxation time T_2 to characterize the influence of the Zeeman decoherence effect phenomenologically. And we find that in the case of overlapping with Zeeman sidebands and the secular motion sidebands, a larger magnetic field results in a larger T_2, thereby increasing the contrast of Ramsey fringes. To avoid the Zeeman decoherence effect, the magnetic field should be more than 150 mGs. But if the magnetic field is too large, it might cause a large second-order Zeeman shift. We have shown that eliminating the Zeeman decoherence effect can definitely obtain better SNR and significantly improve the performance of the $^{199}Hg^{+}$ ion microwave clock.

Acknowledgement

Project supported by the National Key Research and Development Program of China (Grant No. 2022YFB3904002).

References

[1] Rovera G D, Bize S, Chupin B, Guéna J, Laurent P H, Rosenbusch P, Uhrich P and Abgrall M 2016 *Metrologia* **53** S81
[2] Panfilo G, Harmegnies A and Tisserand L 2014 *Metrologia* **51** 285
[3] Mei G H, Zhao F, Qi F, Zhong D, An S F, Wang P F, Ming G, Wang F, Qiu Z J, Kang S B, Wang Q, Wu H H, Yan S D, Hou L S, Wang C and Wang L 2021 *Sci. Sin.-Phys. Mech. Astron.* **51** 019512
[4] Ely T A, Burt E A, Prestage J D, Seubert J M and Tjoelker R L 2018 *IEEE Trans. Ultrason. Ferroelect. Freq. Contr.* **65** 950
[5] Prestage J D, Dick G J and Maleki L 1989 *J. Appl. Phys.* **66** 1013
[6] Prestage J D, Tjoelker R L and Maleki L 1999 *Proceedings of the* 1999 *Joint Conference of the European Frequency and Time Forum and IEEE International Frequency Control Symposium (EFTF/IFCS),* April 13–16, 1999, Besancon, France, p. 121
[7] Prestage J D, Chung S K, Thompson R J and MacNeal P 2009 2009 *IEEE International Frequency Control Symposium Joint with the* 22*nd European Frequency and Time forum*, April 20–24, 2009, Besancon, France, p. 54
[8] Burt E A, Taghavi S, Prestage J D and Tjoelker R L 2008 *IEEE International Frequency Control Symposium*, May 19–21, 2008, Honolulu, USA, p. 371
[9] Tjoelker R L, Prestage J D and Maleki L 1999 *Proceedings of the* 31*st Annual Precise Time and Time Interval Systems and Applications Meeting*, December 7–9, 1999, California, USA, p. 597
[10] Burt E A, Prestage J D, Tjoelker R L, Enzer D G, Kuang D, Murphy D W, Robison D E, Seubert J M, Wang R T and Ely T A 2021 *Nature* **595** 43
[11] Sinuco-Leon G A, Mas H, Pandey S, Vasilakis G, Garraway B M and von Klitzing W 2021 *Phys. Rev. A* **104** 033307
[12] Shuker M, Firstenberg O, Sagi Y, Ben-kish A, Davidson N and Ron A 2008 *Phys. Rev. A* **78** 063818
[13] Wang X C, Cheng H D and Liu L 2012 *Chin. Opt. Lett.* **10** 100201
[14] Santarelli G, Laurent Ph, Lemonde P, Clairon A, Mann A G, Chang S, Luiten A N and Salomon C 1999 *Phys. Rev. Lett.* **82** 4619
[15] Meier F and Loss D 2005 *Phys. Rev. B* **71** 094519
[16] Golter D A and Wang H 2014 *Phys. Rev. Lett.* **112** 116403
[17] Huang P, Kong X, Zhao N, Shi F Z, Wang P F, Rong X, Liu R B and Du J F 2011 *Nat. Commun.* **2** 570
[18] Prestage J D, Tjoelker R L and Maleki L 2001 *Topics Appl. Phys.* **79** 195
[19] Tjoelker R L, Prestage J D and Maleki L 1992 *TDA Progress Report* 42-108, February 15, 1992, Pasadena, USA, p. 19
[20] Liu H, Chen Y H, Yan B B, Liu G and She L 2020 *China Satellite Navigation Conference (CSNC)* 2020 *Proceedings* p. 557
[21] Burt E A, Diener W A and Tjoelker R L 2008 *IEEE Trans. Ultrason. Ferroelect. Freq. Contr.* **55** 2586
[22] Prestage J D, Tjoelker R L, Dick G J and Maleki L 1993 *IEEE International Frequency Control Symposium,* June 2–4 1993, Salt Lake City, USA, p. 148
[23] Demtröder W 2003 *Laser Spectroscopy*, 3rd edn. (Berlin: Springer-Verlag) p. 679
[24] Wang Y Q 1986 *Principle of quantum frequency standards* (Beijing: Science Press) p. 302 (in Chinese)
[25] Cutler L S, Giffard R P and McGuire M D 1985 *Appl. Phys. B* **36** 137